PERGAMON

International Journal of Heat and Mass Transfer 45 (2002) 697–700

International Journal of HEAT and MASS TRANSFER

www.elsevier.com/locate/ijhmt

Technical Note

Radiative heat transfer in absorbing–emitting–scattering gray medium inside 1-D gray Cartesian enclosure using the collapsed dimension method

Subhash C. Mishra [a,*], Manohar Prasad [b]

[a] Department of Mechanical Engineering, Indian Institute of Technology, Guwahati 781 039, India
[b] Department of Mechanical Engineering, Indian Institute of Technology, Kanpur 208 016, India

Received 28 May 2000

1. Introduction

In the present paper, usage of the collapsed dimension method (CDM) [1–3] is extended for solving radiative heat transfer problems in an anisotropically scattering gray planar medium inside 1-D gray Cartesian enclosure. In earlier works [1–3], CDM has been shown to work successfully for radiative transfer problems in 2-D rectangular enclosures with absorbing–emitting medium.

In CDM, 3-D radiative information are collapsed to the 2-D solution plane in terms of effective intensity and optical thickness coefficient. As all the radiative information are collapsed to the 2-D solution plane, the governing equations in CDM are completely different from rest of the numerical methods available for solving radiative heat transfer problems. In this method, as effective intensities are confined to the 2-D plane, like other methods, solid angle does not come into the picture and this greatly reduces both the complexity and the computational expense involved in the solution of radiative transfer problems.

2. Formulation

In a participating medium, at any point on the control surface with optical depth τ, in CDM, radiative heat flux q due to a semi-circle of effective intensities I is given by

$$q(\tau) = \int_0^{\pi} I(\tau,\alpha)\sin\alpha\,\mathrm{d}\alpha, \tag{1}$$

where α is a planar angle, which is defined only in the 2-D plane and is measured from the control surface. In CDM, effective intensity is confined to the 2-D plane and is thus defined as the energy flow rate per unit projected area in the effective intensity direction α per unit planar angle $\mathrm{d}\alpha$,

$$I(\alpha) = \frac{\delta\dot{Q}}{\mathrm{d}A\sin\alpha\,\mathrm{d}\alpha}. \tag{2}$$

In Eq. (1), effective intensity at any optical depth τ is given by

$$I(\tau,\alpha) = I(0,\alpha)\exp(-\tau\eta) + \int_0^{\tau} S(\tau',\alpha)\exp\{-(\tau-\tau')\eta\}\,\mathrm{d}(\tau'\eta), \tag{3}$$

where $I(0,\tau)$ is the boundary effective intensity at $\tau = 0$ and η is the optical thickness coefficient. For a boundary wall having temperature T_w and emissivity ϵ_w, this boundary effective intensity is given by

$$I(0,\alpha) = \underbrace{\epsilon_w\frac{\sigma T_w^4}{2}}_{\text{emitted}} + \underbrace{\frac{1-\epsilon_w}{2}\int_{\alpha=0}^{\pi} I(\alpha)\sin\alpha\,\mathrm{d}\alpha}_{\text{reflected}}. \tag{4}$$

In Eq. (3), S is the source function, and it is given by

$$S(\tau,\alpha) = (1-\omega)I_b(\tau) + \frac{\omega}{2\pi}\int_{\alpha'=2\pi} I(\tau,\alpha')p(\alpha'\to\alpha)\,\mathrm{d}\alpha', \tag{5}$$

where ω is the scattering albedo, I_b is the blackbody effective intensity function [4] which is related to

* Corresponding author. Tel.: +91-361-690-321; fax: +91-361-690-762.

E-mail addresses: scm@iitg.ernet.in (S.C. Mishra), manohar@iitk.ac.in (M. Prasad).

PII: S 0 0 1 7 - 9 3 1 0 (0 1) 0 0 1 5 3 - 3

temperature as $I_b = \sigma T^4/2$ and $p(\alpha' \to \alpha)$ is the scattering phase function. For linear anisotropic phase function, in CDM, it is given by

$$p(\alpha' \to \alpha) = 1 + a_1 \sin\alpha \sin\alpha', \quad (6)$$

where in Eq. (6), a_1 is the anisotropy factor and its value lies in the range $-1 \leqslant a_1 \leqslant 1$. By substituting for $p(\alpha' \to \alpha)$ from Eq. (6) into Eq. (5), we get

$$S(\tau,\alpha) = (1-\omega)I_b(\tau) + \frac{\omega}{2\pi}\int_{2\pi} I(\tau,\alpha')\,d\alpha' + \frac{a_1\omega}{2\pi} \times \sin\alpha \int_{2\pi} I(\tau,\alpha')\sin\alpha'\,d\alpha' \quad (7)$$

which in terms of heat flux q and effective incident radiation G becomes

$$S(\tau,\alpha) = (1-\omega)I_b(\tau) + \left(\frac{\omega}{2\pi}\right)G(\tau) + \left(\frac{a_1\omega}{2\pi}\sin\alpha\right)q(\tau), \quad (8)$$

where in the above equation, effective incident radiation

$$G = \int_{2\pi} I(\tau,\alpha)\,d\alpha. \quad (9)$$

It should be noted that in Eq. (8), q is the net heat flux and is found by extending the integration limit in Eq. (1) from $\alpha = 0,\pi$ to $\alpha = 0, 2\pi$.

In CDM, divergence of the radiative heat flux is given by

$$\nabla \cdot q = \kappa_a \eta [2\pi I_b - G]. \quad (10)$$

In the absence of conduction and convection, in any control volume, emission and absorption are balanced, and thus, the system is said to be in radiative equilibrium. In this situation, $\nabla \cdot q = 0$ and, therefore, I_b, hence temperature T_b, is related to G as

$$I_b(\tau) = \frac{\sigma T_b^4}{2} = \frac{G(\tau)}{2\pi}. \quad (11)$$

In CDM, in radiative equilibrium situation, Eq. (11) is used to find the unknown medium temperature. Therefore, for radiative equilibrium, expression for the source function (Eq. (8)) simplifies to

$$S(\tau,\alpha) = I_b(\tau) + \left(\frac{a_1\omega}{2\pi}\sin\alpha\right)q(\tau). \quad (12)$$

For finding heat flux and temperature information using Eqs. (1) and (11), in CDM, finite number of effective intensities are used. For a finite number of effective intensities, Eqs. (1) and (9) are numerically integrated as

$$q = \left[\int_0^{\pi} I(\alpha)\sin\alpha\,d\alpha\right] = \left[\sum_{n=1}^{N} c_n I(\alpha_n)\right], \quad (13)$$

$$G = \left[\int_0^{2\pi} I(\alpha)\,d\alpha\right] = \left[\sum_{n=1}^{2N} I(\alpha_n)\,\Delta\alpha_n\right], \quad (14)$$

where N is the number of effective rays over a semi-circle and

$$c_n = \left|\cos\left(\alpha_n + \frac{\Delta\alpha_n}{2}\right) - \cos\left(\alpha_n - \frac{\Delta\alpha_n}{2}\right)\right|. \quad (15)$$

In Eq. (15), $|\cdot|$ indicates the absolute value, and the term $\Delta\alpha_n$ is the angle over which the nth effective intensity $I(\alpha_n)$ is acting.

To provide effective intensity information in Eqs. (13) and (14), Eq. (3) is used in the following form:

$$I_{i+1} = I_i \exp(-\tau\eta) + S[1 - \exp(-\tau\eta)], \quad (16)$$

where I_{i+1} is the downstream effective intensity in α direction at any optical depth τ and I_i is the upstream effective intensity in the same direction α. The optical path-leg between the upstream and the downstream points is τ. Eq. (16) is obtained from Eq. (3) with the assumption that for the short optical path-leg between the points $i+1$ and i, the source function given by Eq. (5) remains constant. For the problem in which the solution is required only in 1-D (for example – planar geometry), this constant value is equal to the average of values of the source functions at the upstream and the downstream points. In any problem, an effective intensity is traced from the boundary. At the boundary, intensity values are calculated from Eq. (4). To arrive at any downstream point in the medium, Eq. (16) is used recursively.

3. Validation studies

For validation of the formulation presented above, radiative heat transfer problem in 1-D Cartesian enclosure containing absorbing, emitting and scattering gray medium is considered. The south and the north boundaries of the enclosure are diffuse gray with emissivities ϵ_S and ϵ_N, respectively. Temperatures of the south and the north boundaries are T_S and T_N, respectively. For the validation studies, two types of problems are considered. In case 1, a boundary emission problem, which is the representative of radiative equilibrium, is considered. In this case, net heat flux remains constant at all optical depths. For different boundary emissivities and anisotropy, variations of net heat flux with optical thickness are found, and the same are compared with the self-generated Monte Carlo solution. In case 2, medium emission problem, which is representative of non-radiative equilibrium situation, is taken up. Here the medium is considered as isothermal and both the boundaries are considered at zero temperature. In this case, heat flux at south boundaries are found, and compared with the exact results taken from [4].

3.1. Boundary emission

In this case, south boundary is at some finite temperature T_S and the north boundary temperature T_N is taken as zero. Medium is absorbing, emitting and anisotropically scattering. In Figs. 1(a)–(d), variations of non-dimensional net heat flux with enclosure optical thickness in the range $[0.0001, 5.0]$ have been shown. For results presented in these figures, non-dimensional heat flux Ψ has been calculated from

$$\text{Non-dimensional heat flux } \Psi = \frac{q_{\text{net}}}{\sigma(T_1^4 - T_2^4)}.$$

In Fig. 1(a), for $\epsilon_S = \epsilon_N = 1.0$, heat flux variations are given for values of phase function anisotropy $a_1\omega$ in the range $[-1, +1]$. Here, for $a_1\omega < 0$, medium is backward scattering, whereas for $a_1\omega > 0$, medium is forward scattering. For $a_1\omega = 0$, medium is isotropically scattering, if $a_1 = 0$ and $\omega \neq 0$. It is absorbing–emitting if $\omega = 0$. However, for radiative equilibrium, absorbing–emitting situation and absorbing, emitting and isotropically scattering situation are identical.

In Fig. 1(b), for $a_1\omega = 0.0$, with south boundary emissivity $\epsilon_S = 0.8$, heat flux variations with optical thickness are given for five different values of the north boundary emissivity $\epsilon_N = 1.0$, 0.8, 0.5, 0.3 and 0.1. In Figs. 1(b) and (c), with $\epsilon_S = 0.8$, heat flux variations are given for $\epsilon_N = 0.5$, 0.8, and 1.0. In Fig. 1(c), results are presented for backward scattering with $a_1\omega = -0.7$, whereas in Fig. 1(d), the same are given for forward scattering with $a_1\omega = +0.7$. In Figs. 1(a)–(d), CDM results with 10 effective intensities are compared with that of the self-generated Monte Carlo results. For all the cases, CDM is found to give a very good comparison.

3.2. Isothermal medium emission

In this case, while the geometry is the same as that for the boundary emission case, the absorbing, emitting, and anisotropically scattering medium is isothermal at temperature T_g and both the bounding walls are black and are at zero temperature. Non-dimensional heat flux has been calculated from the following:

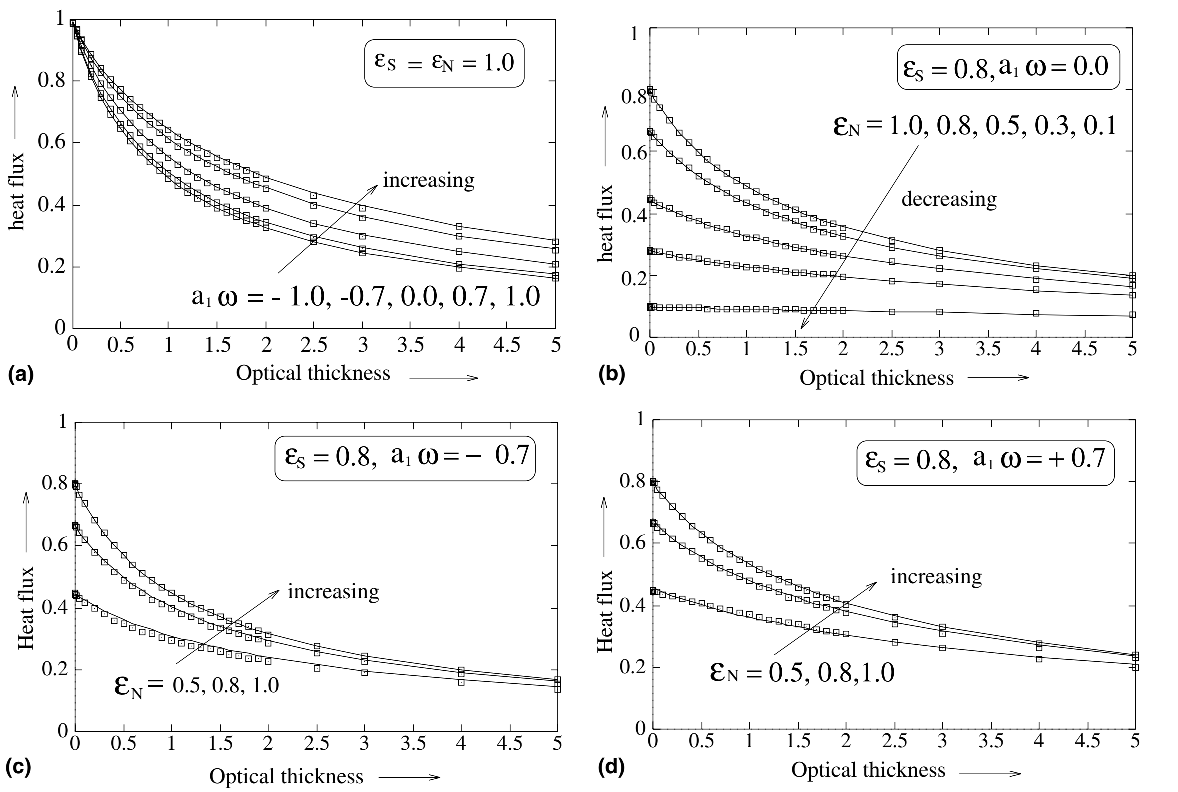

Fig. 1. Variation of non-dimensional net heat flux Ψ with enclosure optical thickness; line – CDM results, markers – Monte Carlo method results [4].

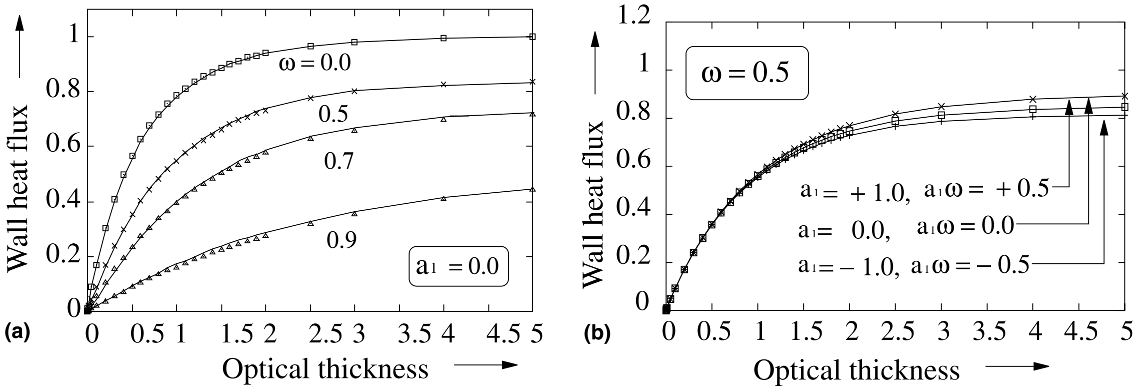

Fig. 2. Variation of non-dimensional wall heat flux Ψ with enclosure optical thickness; line – CDM results, markers – Monte Carlo method results [4].

Non-dimensional heat flux $\Psi = \frac{q_{\text{net}}}{\sigma T_g^4}$.

In Figs. 2(a) and (b), non-dimensional wall heat flux Ψ results calculated from the CDM using 10 effective intensities, have been compared with the exact results [4]. In both the figures, heat flux variations are for optical thickness in the range $[0.0001, 5.0]$. In Fig. 2(a), for $a_1 = 0$, results have been presented for $\omega = 0.0$, 0.5, 0.7, and 0.9. In Fig. 2(b), for $\omega = 0.5$, the same are given for $a_1\omega = -0.5$, 0, and $+0.5$. As is obvious from both the figures, CDM results compare very well with that of the exact results.

4. Conclusions

In the present work, application of the CDM has been extended for radiative heat transfer problems in absorbing, emitting and anisotropically scattering medium. To validate the formulation, in 1-D gray Cartesian enclosure, boundary emission and isothermal medium emission problems have been considered. These are representatives of radiative and non-radiative equilibrium cases, respectively. For both types of problems, over a wide range of enclosure optical thickness, effects of scattering albedo, phase function anisotropy and bounding walls emissivities on non-dimensional wall heat flux have been investigated. For all the test cases, CDM results have been found to compare exceedingly well with the results of the benchmark methods.

References

[1] D.A. Blank, The Cartesian collapsed-dimension method for use in numerical 2-D radiative calculations in absorbing–emitting media, Int. J. Numer. Meth. Eng. 37 (1994) 3023–3036.

[2] D.A. Blank, S.C. Mishra, Use of the 2-D collapsed dimension method in absorbing–emitting media with isotropic scattering, in: Proceedings of the First International Symposium on Radiative Heat Transfer, Kusadasi, Turkey, August 1995, pp. 138–151.

[3] D.A. Blank, S.C. Mishra, Use of the 2-D collapsed dimension method in gray enclosures with absorbing–emitting–isotropic scattering media in radiative equilibrium, Numer. Heat Transfer B 30 (4) (1996) 469–481.

[4] S.C. Mishra, A novel computational approach for the solution of radiative heat transfer problems in participating media, Ph.D. Thesis, IIT Kanpur, India, 1997.